R. Sundberg, and S. Adler-Golden, Effects of the Atmospheric Compensation Method on Hyperspectral Rare Target Detection,10th Workshop on Hyperspectral Imaging and Signal Processing: Evolution in Remote Sensing (WHISPERS) (2019).

See next page for full paper.

EFFECTS OF THE ATMOSPHERIC COMPENSATION METHOD ON HYPERSPECTRAL RARE TARGET DETECTION

Robert Sundberg and Steve Adler-Golden

Spectral Sciences, Inc., 4 Fourth Ave., Burlington, MA 01803

ABSTRACT

This study examines how hyperspectral rare target detection performance is affected by the method of atmospheric compensation used to convert the data to reflectance units. Rare and subpixel target detection algorithms employ contrast enhancement methods to suppress signatures from the background materials. Therefore, when evaluating atmospheric compensation methods, it is important to consider their accuracy in contrast-enhanced space. In particular, a key requirement for good detection is the suppression of atmospheric band residuals in the reflectance spectra, making them as smooth as possible. This explains the success of the empirical Quick Atmospheric Correction (QUAC) algorithm and the importance of supplementing first principles methods with spectral polishing. We illustrate these findings using two data sets acquired by the Rochester Institute of Technology (RIT), three different whitening-based detection algorithms, and three different atmospheric compensation algorithms, QUAC, FLAASH and ATCOR.

Index Terms**—** Spectral, hyperspectral, atmospheric compensation, target detection

1. INTRODUCTION

One of the most valuable uses of hyperspectral imagery is for detection and identification of spectrally unique materials. To mitigate effects due to the atmosphere, detection algorithms typically work with atmospherically compensated (or "corrected") data and target spectra in reflectance units. Detection performance depends on many factors, including target spectral signature contrast and structure, the scene backgrounds, and the accuracy with which the atmospheric contributions have been modeled and removed from the data. The fidelity of the atmospheric compensation is always a concern. There may be errors due to incomplete knowledge of the atmospheric composition, uncertainty in the sensor's optical characteristics, or approximations in the compensation method itself, any of which can lead to small atmospheric band residuals in the retrieved reflectances.

Detection algorithms, especially those used for rare or subpixel targets, employ contrast enhancement methods, such as covariance whitening or subspace projection, to suppress signatures from the background materials. Since the backgrounds tend to be spectrally smooth, the contrast enhancement effect is somewhat similar to that of a high-pass filter, where fine spectral features of the target are preserved while broader, smoother features from the backgrounds are suppressed. When comparing atmospheric compensation methods for detection applications, it is important to consider their accuracy in contrast-enhanced space. This may not be well described by typical criteria such as RMS or spectral angle error.

In this report we evaluate target detection performance with two visible through short-wave infrared (VSWIR) hyperspectral images acquired in different experimental programs under the direction of the Rochester Institute of Technology (RIT) Center for Imaging Sciences. One image is the publicly available detection self-test image taken in 2006 with an airborne HyMap sensor over Cook City, MT (http://dirsapps.cis.rit.edu/blindtest/). The other image was taken in 2016 with an airborne ProSpecTIR sensor over the RIT campus (E. Ientilucci, private communication). Both the scenes have embedded targets with ground truth spectra, a diversity of manmade materials, and mainly vegetated natural backgrounds. We analyzed the images using several different atmospheric compensation processes and detection algorithms, and correlated the results to measures of spectral accuracy. A partial summary of our results for the self-test image appears in an atmospheric compensation review paper in press [1].

2. ATMOSPHERIC COMPENSATION ALGORITHMS

The provided datasets contain both the original radiance data and ATCOR-processed reflectance data cubes [2]. For comparison to these reflectance results we processed the radiance data with a standalone version of QUAC [3] and with the FLAASH [4] algorithm supplied with the ENVI® software package (Harris Corp.). QUAC is an empirical algorithm that doesn't require a priori inputs. The baseline FLAASH compensation was performed with the MODTRAN mid-latitude summer atmosphere, a 7-channel polishing width, and defaults for the remaining settings.

ATCOR and FLAASH are first-principles algorithms based on MODTRAN™ [5] radiation transport calculations. Both algorithms provide spectral polishing options, which improve the spectral smoothness of the retrievals using a linear or affine transform developed from in-scene spectra. The basic polishing concept was introduced by Boardman [6], and his EFFORT method is available in ENVI®. ATCOR offers a choice of several different polishing methods [7]. FLAASH provides a single method based on a running spectral average with a user-adjustable width [8]. The 2016 RIT campus image was atmospherically compensated using ATCOR followed by SpecTIR's proprietary polishing and "virtual empirical line" methods.

To provide additional atmospheric compensation comparisons, we turned off FLAASH's native polishing and added a new post-processing polishing step. As in FLAASH's native method, the reflectance spectra are smoothed with a running average, the smoothed and original spectra are compared to derive a polishing factor, and the factor is applied to the scene. However, the new algorithm de-weights extreme values in a second application of the running average, and also allows the polishing factor to vary in the cross-track direction to compensate for possible variations in sensor response and atmospheric effects across the field of view.

As described in detail elsewhere [3], the QUAC algorithm works by matching an average of diverse, non-vegetated spectra from the scene to an average of diverse reflectance spectra measured in the laboratory. This thoroughly eliminates scene-wide atmospheric effects, making the spectra as smooth as possible and essentially independent of the atmospheric condition and the sensor characteristics. There is no direct correspondence of the materials selected from the scene and the library. However, it is empirically observed that the scene endmember reflectance average and the library endmember average are similar as long as the scene has reasonable surface variety.

3. TARGET DETECTION METHODS

For the self-test scene, we ran each of the above three atmospheric compensation processes with three different target detection algorithms on the subpixel targets. The first detection algorithm is the standard ACE detector [9]. For the ACE score one may choose any of various monotonically related quantities, including spectral angle or trigonometric functions thereof, in de-meaned, covariance-whitened data space [10]. The other two detectors are locally adaptive variants of ACE that are suitable for single-pixel or subpixel targets. One, denoted LM-ACE, is the locally de-meaned detector described in Cohen et al. [11]; the de-meaning kernel is 3x3 pixels. The other, denoted LV-ACE, adds the further step of whitening the local variance (i.e., the covariance matrix diagonal) within a 7x7 kernel. For the RIT campus scene we ran only the ACE detector, since the targets are multiple-pixel.

Due to very strong atmospheric absorption, certain spectral bands, labeled "bad" bands, are poorly retrieved or contain little useful information, and should be excluded from the analysis. We used the same "bad band" lists for all atmospheric compensation methods. Problems can occur in the data whitening step if the covariance matrix is computed from an insufficient number of data points (i.e., pixels) or has less than full rank; the latter occurs if "good" bands have been replicated or interpolated. To avoid these problems, we regularized the covariance matrices using the Oracle Approximating Shrinkage method [12].

3. RESULTS

Self-Test Image. The HyMap self-test image, shown in Figure 1, contains a number of multiple-pixel and full pixel fabric and vehicle targets. The full dataset [13] includes ground-truth spectra and nominal "truth" regions of interest (ROIs) for each target. We focused on the four subpixel targets, as they are more difficult to detect and their results are more straight forward to interpret. Once the targets were definitively located, we were able to refine the ROI locations by applying small shifts of up to a few pixels. For one of the targets, vehicle V2, the ROI was uncertain, so we have omitted those results. The measured target reflectance spectra are shown in Figure 2. Target V1 is a white vehicle, F3 is a blue cotton fabric and F4 is a red nylon fabric.

Figure 1. The RIT Target Detection Self-Test scene in true color.

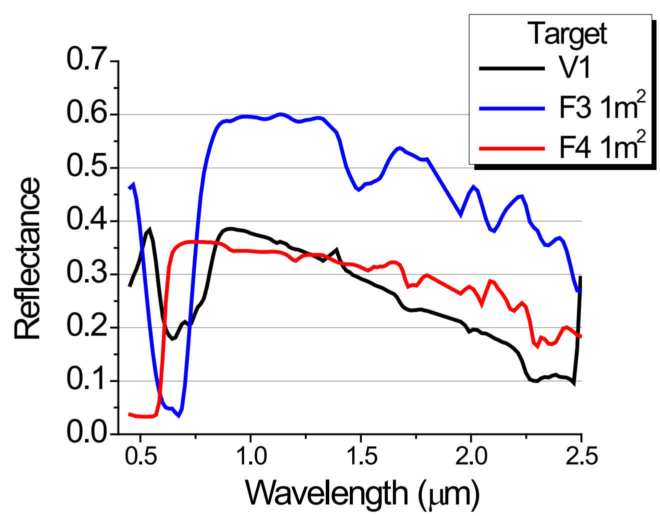

Figure 2. Spectral reflectance for targets used in this study.

A summary of our results is shown in Table 1, given as the number of false positives in detecting the target pixel. The subpixel fabric targets F3 and F4 are also present as full-pixel emplacements, resulting in over-counting the false positives by up to several counts. Detection algorithms give different results depending on the atmospheric compensation algorithm used. The best performance with the ACE detector is with the empirical QUAC algorithm, while the updated polishing technique applied to FLAASH gives the best performance for the two locally adaptive variants of ACE. The best results for each target and detector are highlighted in red in Table 1.

In Figure 3 we show the spectral angle (SA) between the three target spectra (Figure 2) and a full target pixel from the atmospherically compensated scenes. Also shown are the same SA results using the whitened target and scene spectra. In both cases we have normalized the SA results by the FLAASH SA results. The ATCOR results generally produce the smallest spectral angle in reflectance space, but when calculating the SA in whitened space QUAC and FLAASH with the new polishing scheme produce the smallest spectral angle and consequently the best detection performance using the ACE detector (see Table 1).

RIT Campus Image. This image is shown in Figure 4. It contains three large tarps, red, green and blue, placed on the grass near a parking area; see Figure 5. In addition to the supplied ATCOR-based reflectance data cube, we compensated the radiance data using FLAASH and QUAC. FLAASH results were generated using the original polishing method and the updated polishing method. Contiguous pixels containing the spectral signature of the green, red and blue targets were selected by hand and assigned as target ROIs. With these sizable ROIs, the number of target-containing pixels is sufficient for generating useful receiver operating characteristic (ROC) curves for detection.

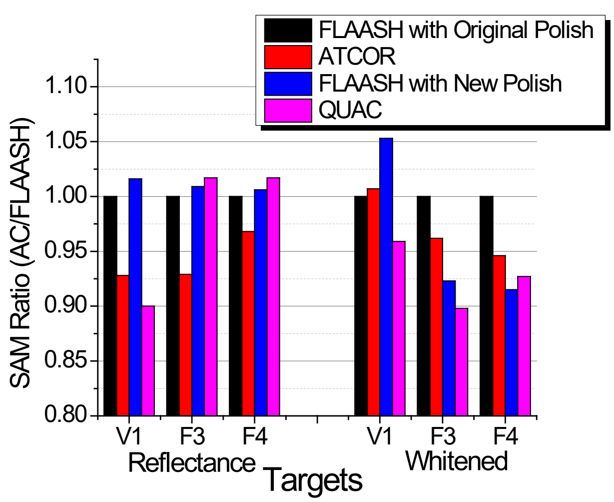

Figure 3. Spectral angle results for different atmospheric compensation approaches normalized to FLAASH SA result.

Table 1. Number of false positives in detecting subpixel targets in the RIT self-test dataset.

Compensation Algorithm	Target	ACE	LM-ACE	LV-ACE
ATCOR	V1	20	2	2
	F3, 1m^2	233	13	15
	F4, 1m^2	110	35	**2**
FLAASH	V1	17	**1**	**1**
	F3, 1m^2	412	**7**	10
	F4, 1m^2	145	48	4
FLAASH with New Polishing	V1	29	**1**	**1**
	F3, 1m^2	143	**7**	**5**
	F4, 1m^2	110	**32**	**2**
QUAC	V1	**3**	2	2
	F3, 1m^2	**99**	**7**	9
	F4, 1m^2	**102**	42	**2**

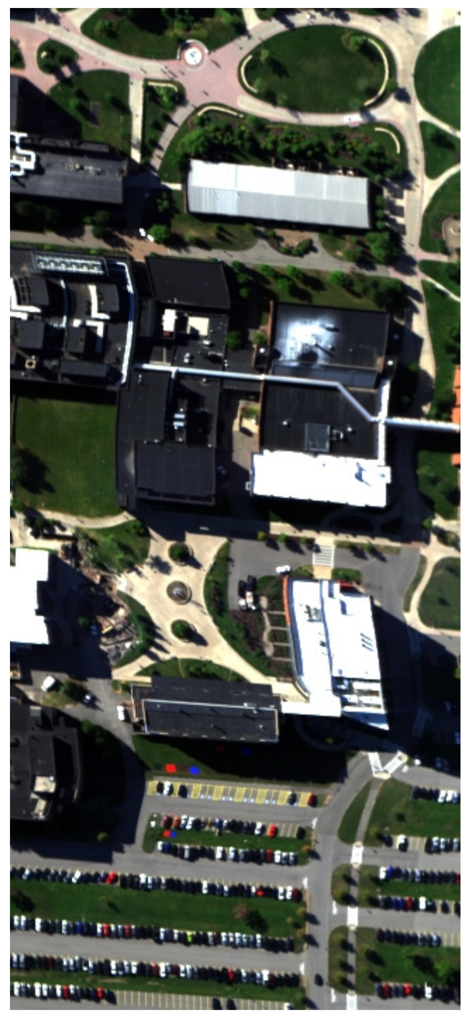

Figure 4. True color reflectance image of ProSpecTIR HSI data of RIT campus and target area.

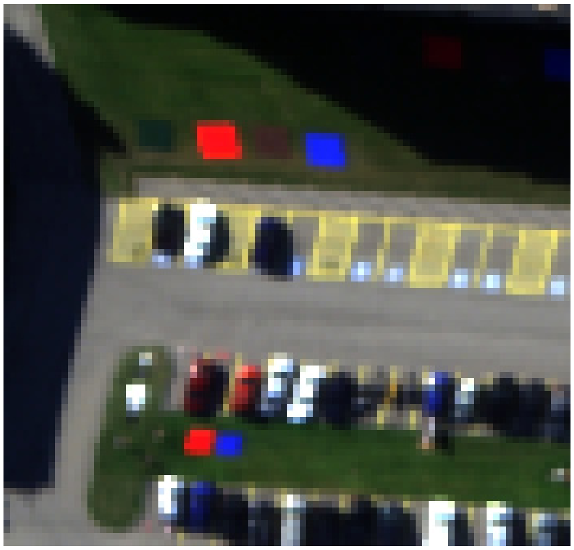

Figure 5. Detail image showing the four-color targets (green, red, brown and blue) placed near the Center for Imaging Science building.

The ROC curves using the ACE detector are shown in Figure 6 for atmospheric compensation with QUAC, FLAASH with the new polishing method, and the ATCOR/SpecTIR method. Once again QUAC is the best performing atmospheric compensation algorithm with ACE detection. The second-best is FLAASH with the updated polishing method.

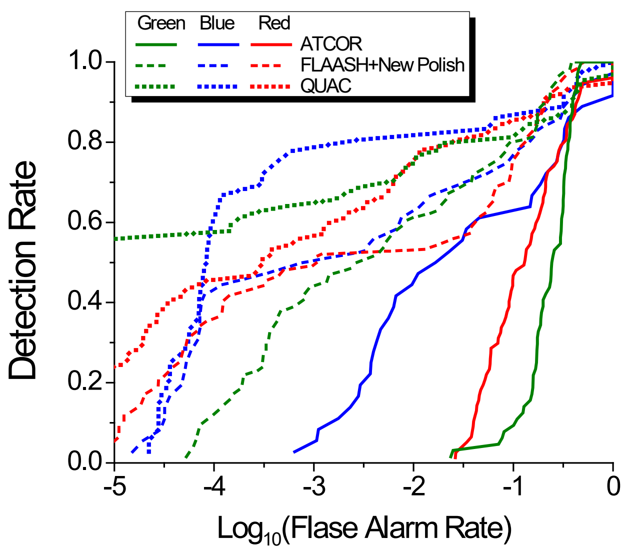

Figure 6. ROC curves for the large sunlit green, blue and red targets using three different atmospheric compensation techniques.

4. CONCLUSIONS

Our results from two VSWIR hyperspectral data sets indicate that rare target detection is strongly affected by the atmospheric compensation method used to retrieve reflectance spectra from the radiance data. The results correlate with retrieval accuracy in whitened space. The empirical Quick Atmospheric Correction (QUAC) algorithm, which is very simple to use, gives surprisingly good results, comparable to or better than those from first-principles atmospheric compensation methods, ATCOR and FLAASH. We ascribe QUAC's success to its enforced spectral smoothness, which provides good signature fidelity in whitened space. We recommend further investigation with a greater variety of images and processing methods, including different methods of covariance regularization and band selection.

ACKNOWLEDGMENT

The authors wish to acknowledge Spectral Sciences, Inc. for support under an internal research and development grant. The authors thank Dr. Emmett Ientilucci, Digital Imaging and Remote Sensing Laboratory, Rochester Institute of Technology, for providing the ProSpecTIR data and for helpful discussions.

5. REFERENCES

[1] Ientilucci, E.J. and S. Adler-Golden, "Atmospheric Compensation of Hyperspectral Data," *IEEE Geoscience and Remote Sensing Magazine*, in press (2019).

[2] Richter, R. and D. Schläpfer, "Geo-atmospheric processing of airborne imaging spectrometry data. Part2: Atmospheric/topographic correction," Int. J. Remote Sensing, vol. 23, pp. 2631–2649 (2002).

[3] Bernstein, L.S., X. Jin, B. Gregor and S.M. Adler-Golden, "Quick atmospheric correction code: algorithm description and recent upgrades," Opt. Eng. 51(11), 111719 (2012).

[4] Perkins, T., S.M. Adler-Golden, M.W. Matthew, A. Berk, L.S. Bernstein, J. Lee and M. Fox, "Speed and accuracy improvements in FLAASH atmospheric correction of hyperspectral imagery," Opt. Eng. 51(11), 111707 doi:10.1117/1.OE.51.11.111707 (2012).

[5] Berk, A., G.P. Anderson, P.K. Acharya, L.S. Bernstein, L. Muratov, J. Lee, M.J. Fox, S.M. Adler-Golden, J.H. Chetwynd,

[6] Boardman, J. W., "Post-ATREM polishing of AVIRIS apparent reflectance data using EFFORT: a lesson in accuracy versus precision," Summaries of the Seventh JPL Airborne Earth Science Workshop, Vol. 1, p. 53 (1998).

[7] Richter, R. and D. Schläpfer, ATCOR-4 User Guide, Version 7.0.3, March 2016.

[8] Adler-Golden, S.M., M.W. Matthew, L.S. Bernstein, R.Y. Levine, A. Berk, S.C. Richtsmeier, P.K. Acharya, G.P. Anderson, G. Felde, J. Gardner, M. Hoke, L.S. Jeong, B. Pukall, J. Mello, A. Ratkowski, and H.-H. Burke, Atmospheric Correction for Short-wave Spectral Imagery based on MODTRAN4, SPIE Proceeding, Imaging Spectrometry V, Volume 3753 (1999).

[9] Kraut, S.S., L.L. Scharf, R.W. Butler, "The Adaptive Coherence Estimator: A Uniformly Most-Powerful Invariant Adaptive Detection Statistic," IEEE Trans. Signal Processing, Vol. 53, No. 2 (2005).

[10] Adler-Golden, S.M. and P. Conforti, "Robust Hyperspectral Detection with Algorithm Fusion," *Proceedings of the 2010 IEEE International Geoscience and Remote Sensing Symposium* (2010).

[11] Cohen, Y., August, Y., Blumberg, D.G. and Rotman, S.R., "Evaluating Subpixel Target Detection Algorithms in Hyperspectral Imagery," J. Electrical Computer Eng., Vol. 2012, ID 103286, 15 pages, doi:10.1155/2012/103286.

[12] Chen, Y., A. Wiesel, Y.C. Eldar and A.O. Hero, "Shrinkage algorithms for MMSE covariance estimation," IEE Trans. Signal Processing, 58, pp. 5016-5029 (2010).

[13] D. Snyder, J. Kerekes, I. Fairweather, R. Crabtree, J. Shive, and S. Hager, "Development of a Web-based Application to Evaluate Target Finding Algorithms," *Proceedings of the 2008 IEEE International Geoscience and Remote Sensing Symposium (IGARSS)*, vol. 2, pp. 915-918, Boston, MA, 2008.